Sensors and Materials, Vol. 32, No. 7 (2020) 2517–2525
MYU Tokyo

S & M 2279

$Pb_{52}(Zr,Ti)_{48}O_3$ Ferroelectric Dipole Electret Exploiting Surface Pillar Array Structure for Electrostatic Vibration Energy Harvesters

Hung Hoang Nguyen,[1,2*] Haruhiko Asanuma,[3] Hiroyuki Oguchi,[1,4]
Gaël Sebald,[5] and Hiroki Kuwano[1,2,5]

[1]New Industry Creation Hatchery Center (NICHe), Tohoku University,
6-6-10 Aramaki-Aoba, Aoba-ku Sendai, Miyagi 980-8579, Japan
[2]Sendai Smart Machine Co., Ltd. (SSM), 6-6-40 Aza-Aoba, Aramaki, Aoba-ku, Sendai, Miyagi 980-8579, Japan
[3]Institute of Science and Engineering, Faculty of Frontier Engineering, Kanazawa University,
Kakuma-machi, Kanazawa 920-1192, Japan
[4]Advanced Institute for Materials Research, Tohoku University,
2-1-1 Katahira, Aoba-ku, Sendai, Miyagi 980-8577, Japan
[5]ELyTMaX UMI 3757, CNRS – Université de Lyon – Tohoku University, International Joint Unit,
Tohoku University, 2-1-1 Katahira, Aoba-ku, Sendai, Miyagi 980-8577, Japan

(Received March 9, 2020; accepted May 18, 2020)

Keywords: ferroelectric dipole electrets, FDE, PZT, vibration energy harvesters, electrets

In this paper, we present ferroelectric dipole electrets (FDEs) with patterned $Pb_{52}(Zr,Ti)_{48}O_3$ (PZT) pillar arrays. Their output power generation capability was higher than that of flat FDEs when used for electrostatic vibration energy harvesters (e-VEHs). This excellent capability was achieved since the patterned pillar structure increased the electric field near the electret surface. The surface potential (V_s) became as high as 1035 V when the surface charge density was 6.9 mC/m^2. This surface charge density was 1.3-fold higher than that of flat FDEs and sixfold higher than that of conventional CYTOP polymer electrets (CPEs). Consequently, VEHs (20 × 20 × 1 mm^3) showed a maximum power of 102 μW at an acceleration of 0.6 g (1 g = 9.8 m/s^2) and a frequency of 20 Hz. These results will open a new strategy for the use of FDEs in e-VEHs.

1. Introduction

Vibration energy harvesters (VEHs) have been considered as potential self-sustainable power sources for the Internet of Things (IoTs).[1–3] In this aspect, among various types of VEH, electrostatic energy harvesters have attracted attention since they can operate under ambient vibration conditions (frequency and acceleration are below 100 Hz and 1.0 g, respectively).[4,5] Their compatibility with MEMS processing[6] is another advantage regarding miniaturization.

One of the main challenges for electrostatic VEHs is to increase their output power generation capability. Responding to this challenge, Asanuma *et al.* developed a new type of electret, named ferroelectric dipole electrets (FDEs), which was a ferroelectric material with

*Corresponding author: e-mail: hung@nanosys.mech.tohoku.ac.jp
https://doi.org/10.18494/SAM.2020.2854

ISSN 0914-4935

a relative permittivity (ε_r) of more than 1000, much higher than that of conventional CYTOP polymer electrets (CPEs, $\varepsilon_r \sim 2.1$).[4,6,7] As a result, the output power of FDE-based VEHs was increased threefold that of CPE-based energy harvesters.[4] However, such an increase was limited because strong electric fields were still trapped inside the FDE; hence, these prototype VEHs effectively used only the fringe electric field at the corner of the FDE.[8] To increase the effective electric field strength, one possible approach is to increase the number of edges.

On the basis of this idea, in this study, we attempted to increase the boundary area of electrets by fabricating a patterned pillar structure on commercial $Pb_{52}(Zr,Ti)_{48}O_3$ (PZT). The effects of the pitch size of the structure on remnant polarization, surface potential, and surface charge density were investigated. We achieved a high surface charge density, which increased sixfold that of CPEs and 1.3-fold that of flat FDEs. The output power generated by the pillar array FDE was measured to confirm the validity of using this structure.

2. Design of Electrets

We firstly simulated the electric fields generated by the patterned and flat (unpatterned) FDEs. The simulation was conducted using COMSOL Multiphysics. For the patterned structure, the dimensions for the simulation were set at $t = w = g = 1$ mm, where t is the electret thickness, w and g are the width of the pillars and the gap between them, respectively. The size of the air domains was set to be much larger than electret dimensions as $10(w + g) \times 10t$.

Surface charge density was set as the remnant polarization of 20 mC/m^2 for both FDEs. The positive charges were placed on the upper surface, while the negative charges were set on the lower surfaces. The surface charges were fixed and could not move on the surface. The simulated y-component of electric fields (E_y) obtained for both the flat (unpatterned) and patterned FDEs are compared in Fig. 1(a). Such a comparison indicated that patterning could enhance the electric field. On the surface of the patterned structure ($d \sim 0$), the strength of the electric field was 1.5×10^6 V/m, 2.5-fold that on the surface of the flat FDE.

Figure 1(b) shows the magnitude of the y-component of electric fields near the center for the two FDEs. The magnitude of the electric field of both FDEs decreased as the distance increased. However, the electric field of the patterned sample degraded much faster than that of the flat FDE. When moving far from the FDE surface, the contribution of the fringe field became negligible.[8] The electric fields of the pillar FDEs were higher up to 922 μm. On the basis of this result, to exploit the advantage of the patterned structure, the oscillator in the energy harvester device should move close to the FDE surface. These simulation results served as a basis for the design of experimental devices.

3. Experimental Procedure

The pillar arrays were fabricated on unpoled hard PZT ceramics (Fuji Ceramics Corp.; No. C-2: $L \times W \times t = 20 \times 20 \times 1.0$ mm^3). In this study, these hard-type ferroelectric materials were selected because they show longer stability of their surface potential.[9] Patterned structures with three different pitch sizes (0.2, 0.5, and 1.0 mm) were prepared using a dicer (DISCO,

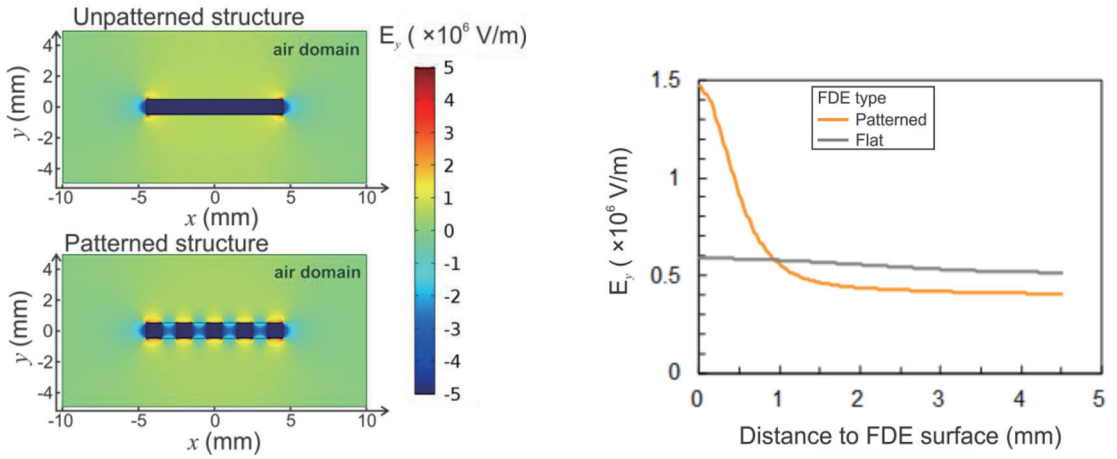

(a) (b)

Fig. 1. (Color online) (a) Electric fields along y-direction (E_y) generated by flat and patterned FDEs and (b) magnitude of E_y at $x = 0$.

DAD3240). We also prepared unpatterned samples (flat FDEs) for the comparison of the FDE performance characteristics.

The pillar PZTs were polarized by applying an external electric field to a pair of Au electrodes in a silicon oil bath.[4] The applied poling electric field and treatment time were 4.0 kV/mm and 1.0 h, respectively. The permittivities of the pillar structures were measured using an impedance analyzer (HP-4194A). The surface potentials of the FDEs were determined using a noncontact electrostatic voltmeter (Trek Inc., Model 344).

After removing the upper electrode and silicon oil, the output power generated by the patterned FDE was measured using the setup shown in Fig. 2. The FDE was placed on a translational stage with the lower electrode and vibrated vertically using a standard shaker (G-Master APD-200FCG). The initial air gap between the FDE surface and the upper electrode was precisely controlled using a micrometer. To measure the displacement of the electret, we vibrated the FDE without the upper electrode and used a laser Doppler vibrometer (Ono-Sokki LV-1710) focused on the surface of the FDE.

The output power was obtained at a frequency of 20 Hz with various initial air gaps, load resistances (R_L), and accelerations (a). The waveform of the output voltage generated from the FDE was obtained using an oscilloscope (Iwatsu, DS-5552). As shown in the inset in Fig. 2, the waveform of the output voltage is not sinusoidal because the capacitance between the upper electrode and the FDE does not change linearly with the air gap during vibration.[4,10,11]

4. Result and Discussion

4.1 FDEs characteristics

We successfully fabricated the pillar arrays with different pitch sizes on FDEs by dicing. Typical SEM images of the pillar arrays fabricated using a 0.5-mm-thick blade are shown in Fig. 3.

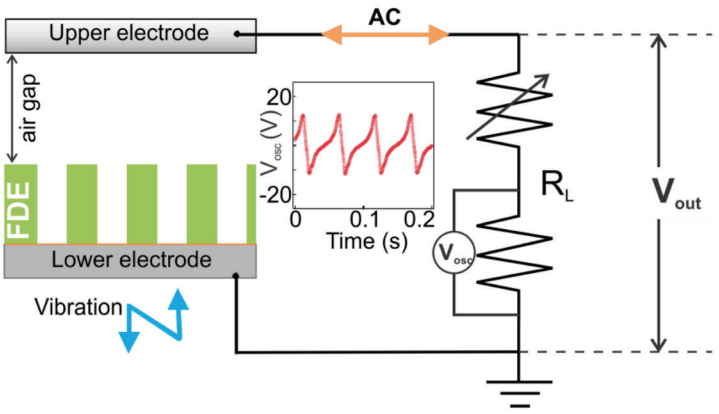

Fig. 2. (Color online) Experimental setup for output power evaluation and the waveform of output voltage generated by our FDEs (inset).

The sizes of the pillar and the pitch (d_p) were designed to be 1.0 × 1.0 × 1.0 mm^3 and 1.5 mm, respectively.

The *P*–*E* hysteresis loops of FDEs with different d_p values of 1.2, 1.5, and 2.0 mm and a flat FDE with a thickness of 1.0 mm, are plotted in Fig. 4. We obtained a similar P_r of 216 mC/m^2 at the applied electric field of 4.0 kV/mm for all samples, indicating that the FDEs are fully polarized. Their surface potential (V_s) and corresponding surface charge density are shown in Fig. 5. The surface potential measured at around 200 μm above the FDE surface was 1035 V for a d_p of 2.0 mm (FDE1). This value was almost twofold higher than that of the flat one (FDE4), consistent with the simulation results.

The surface charge density of the FDEs was calculated as $\sigma = (\varepsilon_r \times \varepsilon_0 \times V_s)/t$, where σ is the surface charge density, ε_r and ε_0 are the relative permittivity of the material and the vacuum permittivity, respectively, V_s is the surface potential, and t is the electret thickness. By using the patterned pillar structure, we obtained the highest σ of 6.9 mC/m^2 with a d_p of 2.0 mm. This σ increased sixfold that of conventional CYTOP.[4,12] Micropower generation using electrets has attracted much attention owing to their large power output in the low frequency range. Since the theoretical power output is proportional to the square of the surface charge density of an electret, the development of a high-performance electret is required. In this study, we show that the surface charge density of a CYTOP electret is significantly improved by the addition of terminal groups. On the basis of this finding, a novel high-performance polymer electret has been developed by doping a silane-coupling reagent into the polymer. A series of measurements of surface potential and thermally stimulated discharge (TSD) showed that they were 1.3-fold higher than those of the flat one. For comparison, we summarized the ferroelectric properties of the FDEs in Table 1. The Curie temperature (T_c) and electromechanical coupling factor (k_p) were provided by the manufacturer (Fuji Ceramics Corp.) for the hard PZT.

4.2 Output power measurement

By using the pillar structures, we successfully enhanced the output power of the FDE. Figure 6 shows the results of initial air gap optimization between the electret and the upper

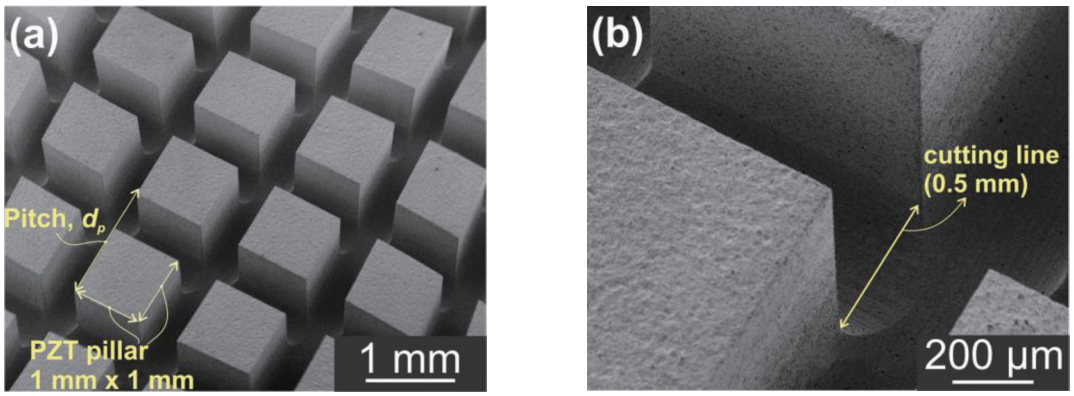

Fig. 3. (Color online) (a) SEM image of FDE composed of PZT pillar arrays with pitch (d_p) of 1.5 mm and (b) enlarged image at cutting lines.

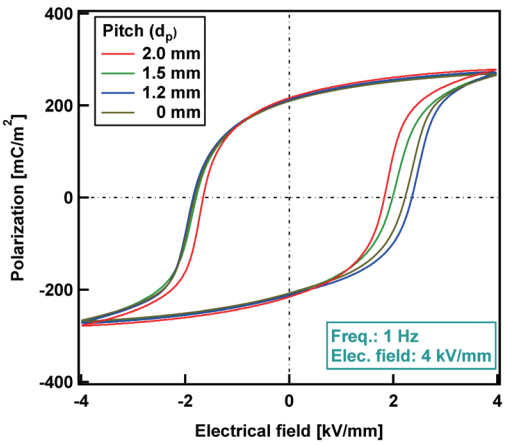

Fig. 4. (Color online) *P*–*E* hysteresis loops of FDEs with different pitches (d_p). The polarization was determined on the effective area of ferroelectric materials. Our FDEs obtained a remnant polarization of 216 mC/m^2.

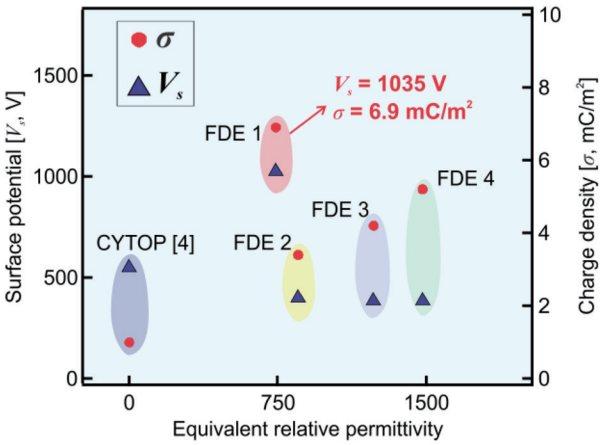

Fig. 5. (Color online) Surface potentials and charge densities of FDEs with different pitches (d_p) [(FDE1 (2.0 mm), FDE2 (1.5 mm), FDE3 (1.2 mm), FDE4 (flat, 0 mm)], and conventional CYTOP.

Table 1
Poling electric field and material characteristics of FDEs and CYTOP.[4] The Curie temperature (T_c) and electromechanical coupling factor (k_p) were provided by the manufacturer for the hard PZT.

	E_{poling} (kV/mm)	V_s (V)	σ (mC/m^2)	ε_r	k_p (%)	T_c (°C)	P_r (mC/m^2)	E_c (kV/mm)
FDE1	**4.0**	**1035**	**6.9**	**740**	**59.6**	**300**	**216**	**1.83**
FDE2	4.0	408	3.4	853	59.6	300	210	1.99
FDE3	4.0	395	4.2	1233	59.6	300	212	2.36
FDE4	4.0	394	5.2	1480	59.6	300	209	2.24
CYTOP[4]	—	559	1.0	2.1	—	—	—	—

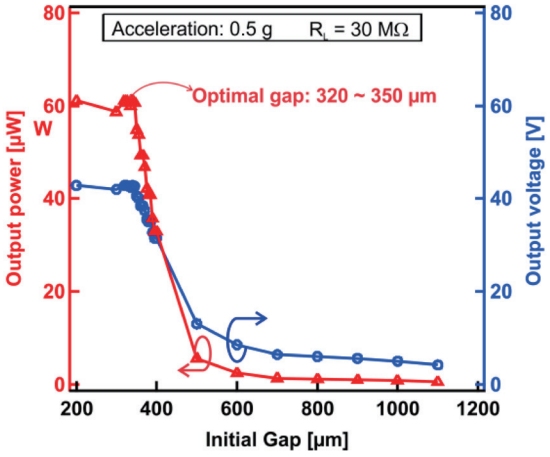

Fig. 6. (Color online) Results of air gap optimization for output power of FDE1. The optimized gap was in the range of 320–350 μm.

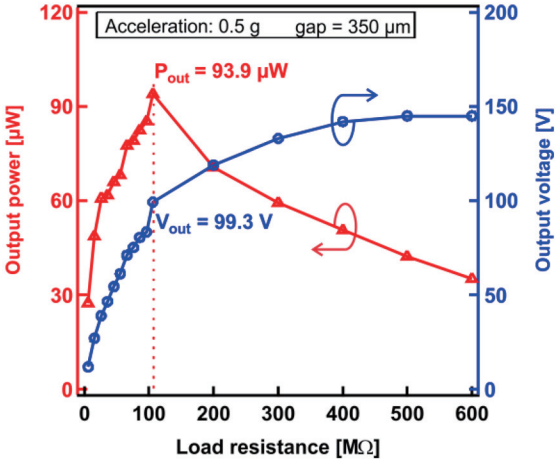

Fig. 7. (Color online) Results of impedance matching for FDE1. The optimal load resistance was 106 MΩ and the output power and voltage were 93.9 μW and 99.3 V, respectively.

electrode for the FDE with a d_p of 2.0 mm (FDE1). The acceleration and load resistance were firstly set at 0.5 g and 30 MΩ, respectively. The highest output power was obtained with an air gap in the range of 320–350 μm. The zero-to-peak displacement of the FDE at an acceleration of 0.5 g was 303 μm; therefore, when the gap became narrower (< 320 μm), the FDE hit the upper electrode and the output power saturated.

Figure 7 shows the dependence of output power on the total load resistance (R_L). The optimized load resistance for the harvester was 106 MΩ. We achieved a high output power of 93.9 μW with a voltage of 99.3 V at an acceleration of 0.5 g, which was almost twofold higher than that of the flat FDE previously reported.[4]

We investigated the dependences of the output power and FDE displacement on the acceleration. The obtained results are plotted in Fig. 8. The initial air gap between the FDE and the upper electrode was set to 350 μm. The displacement of the FDE was measured without the upper electrode. The output power increased monotonically to 102 μW as the acceleration increased up to 0.6 g. At an acceleration of 0.6 g, the zero-to-peak displacement of the FDE was 346 μm. At an acceleration of more than 0.6 g, the output power saturated since the FDE hit the upper electrode.

To evaluate the performance of a VEH, the output power density should be considered. The output power density is defined as the output power normalized by the total volume of the electret and air gap. Figure 9 shows the power densities of VEHs using electrets for power generation. Our VEH with an FDE provided a power density of 189 μW/cm^{-3}, which is higher than most of the power densities of the VEHs, and close to the power densities of the best CPEs or polytetrafluoroethylene (PTFEs) using in-plane structures.[12,13] Possibly, the output power density can be further improved by our FDEs if the in-plane structures are used.

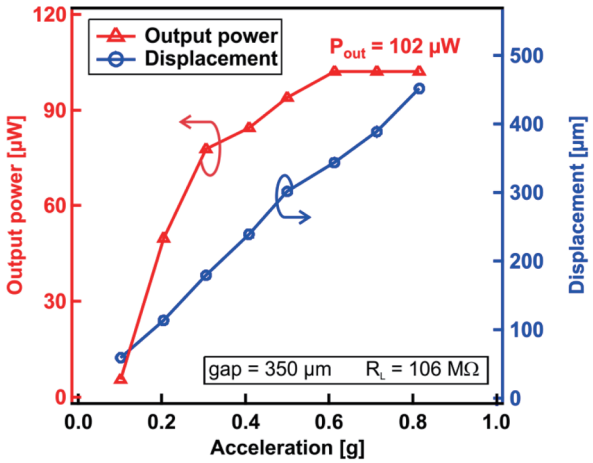

Fig. 8. (Color online) Dependences of output power and FDE displacement on acceleration. The FDE generated a maximum output power of 102 μW at 0.6 g with a load resistance of 106 MΩ.

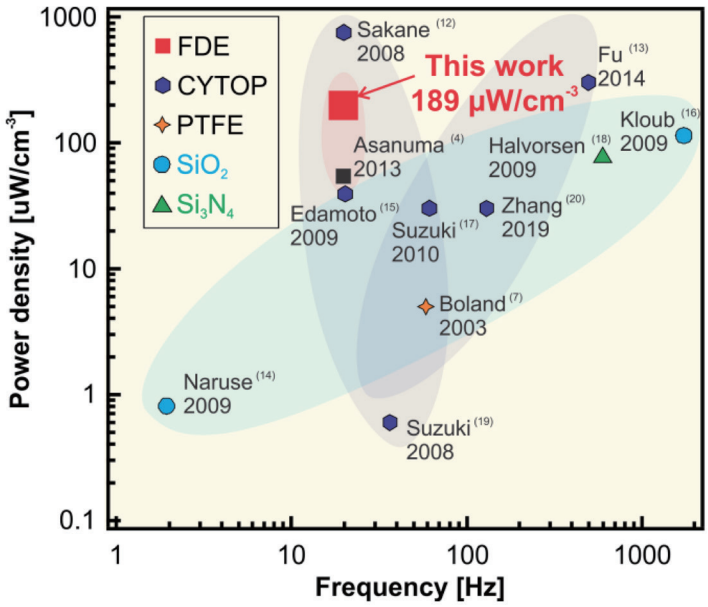

Fig. 9. (Color online) Power densities of this work and state-of-the-art electret-based VEHs. The volume for power density calculation is the total volume of the electret and air gap.[4,7,12–20]

5. Conclusions

We successfully developed the pillar array structures of PZT FDEs. The electrets showed a superior performance to a flat FDE and CPEs. The FDEs with patterned pillar arrays showed three- and sixfold increases in surface charge density in comparison with the flat FDE and CPEs, respectively. Consequently, the output power of VEHs with a patterned pillar-based FDE was almost 200% higher than that of the VEH with a flat FDE and comparable to the highest

value reported for CPEs/PTFEs. The result obtained in this work confirmed the validity of our microstructuring approach and will facilitate the use of ferroelectric materials as electrets in electrostatic VEHs.

Acknowledgments

This work was supported by the JKA Social Action Program. We would like to thank Dr. LE VAN MINH of New Industry Creation Hatchery Center (NICHe), Tohoku University, for his supports in establishing the fabrication technique of patterned FDEs.

References

1 F. Narita and M. Fox: Adv. Eng. Mater. **20** (2018) 1700743. https://doi.org/10.1002/adem.201700743
2 H. Kuwano, L. Van Minh, H. H. Nguyen, H. Asanuma, and H. Oguchi: Proc. 2018 IEEE/ASME Int. Conf. Advanced Intelligent Mechatronics (AIM) 395. https://doi.org/10.1109/AIM.2018.8452279
3 H. H. Nguyen, H. Oguchi, L. Van Minh, and H. Kuwano: ACS Comb. Sci. **19** (2017) 365. https://doi.org/10.1021/acscombsci.6b00193
4 H. Asanuma, H. Oguchi, M. Hara, R. Yoshida, and H. Kuwano: Appl. Phys. Lett. **103** (2013) 162901. https://doi.org/10.1063/1.4824831
5 S. Roundy, P. K. Wright, and J. Rabaey: Comput. Commun. **26** (2003) 1131. https://doi.org/10.1016/S0140-3664(02)00248-7
6 H. Asanuma, M. Hara, H. Oguchi, and H. Kuwano: AIP Adv. **6** (2016) 075206. https://doi.org/10.1063/1.4958884
7 J. Boland, Yuan-Heng Chao, Y. Suzuki, and Y. C. Tai: Proc. Sixteenth Annu. Int. Conf. Micro Electro Mechanical Systems (MEMS) (2003) 538. https://doi.org/10.1109/MEMSYS.2003.1189805
8 G. W. Parker: Am. J. Phys. **70** (2002) 502. https://doi.org/10.1119/1.1463738
9 H. Asanuma, H. Oguchi, M. Hara, and H. Kuwano: J. Phys. Conf. Ser. **476** (2013) 012041. https://doi.org/10.1088/1742-6596/476/1/012041
10 S. Boisseau, G. Despesse, T. Ricart, E. Defay, and A. Sylvestre: Smart Mater. Struct. **20** (2011). https://doi.org/10.1088/0964-1726/20/10/105013
11 Y. Chiu and Y. C. Lee: J. Micromech. Microeng. **23** (2013). https://doi.org/10.1088/0960-1317/23/1/015012
12 Y. Sakane, Y. Suzuki, and N. Kasagi: J. Micromech. Microeng. **18** (2008) 104011. https://doi.org/10.1088/0960-1317/18/10/104011
13 Q. Fu and Y. Suzuki: Proc. The IEEE Int. Conf. Micro Electro Mechanical Systems (MEMS) (2014) 409. (Institute of Electrical and Electronics Engineers Inc., 2014). https://doi.org/10.1109/MEMSYS.2014.6765663
14 Y. Naruse, N. Matsubara, K. Mabuchi, M. Izumi, and S. Suzuki: J. Micromech. Microeng. **19** (2009) 094002. https://doi.org/10.1088/0960-1317/19/9/094002
15 M. Edamoto, Y. Suzuki, N. Kasagi, K. Kashiwagi, Y. Morizawa, T. Yokoyama, T. Seki, and M. Oba: Proc.2009 IEEE 22nd Int. Conf. Micro Electro Mechanical Systems (2009) 1059. https://doi.org/10.1109/MEMSYS.2009.4805569
16 H. Kloub German, D. Hoffmann, B. Folkmer, H. Kloub, and Y. Manoli: Proc. 2009 9th Int. Conf. Micro and Nanotechnology for Power Generation and Energy Conversion Applications (PowerMEMS2009) 165.
17 Y. Suzuki, D. Miki, M. Edamoto, and M. Honzumi: J. Micromech. Microeng. **20** (2010) 104002. https://doi.org/10.1088/0960-1317/20/10/104002
18 E. Halvorsen, E. R. Westby, S. Husa, A. Vogl, N. P. Ostbo, V. Leonov, T. Sterken, and T. Kvisteroy: Proc. TRANSDUCERS 2009–2009 Int. Solid-State Sensors, Actuators and Microsystems Conf. (2009) 1381. https://doi.org/10.1109/SENSOR.2009.5285829
19 Y. Suzuki, M. Edamoto, N. Kasagi, K. Kashiwagi, Y. Morizawa, T. Yokoyama, T. Seki, and M. Oba: Proc. 2008 The 8th International Conference on Micro and Nanotechnology for Power Generation and Energy Conversion Applications (PowerMEMS2008) 7.
20 Y. Zhang, Y. Hu, M. Wang, and F. Wang: Proc. 2019 IEEE 32nd Int. Conf. Micro Electro Mechanical Systems (MEMS) 1013. https://doi.org/10.1109/MEMSYS.2019.8870794

About the Authors

Hoang Hung Nguyen received his B.Sc. and M.Sc. degrees from Hanoi University of Science and Technology, Vietnam, in 2010 and 2012, respectively. He obtained his Ph.D. degree from Tohoku University, Japan, in 2018. From 2018 to 2019, he was a postdoctoral fellow at Tohoku University, Japan. Since 2019, he has been a researcher in Sendai Smart Machine Co., Ltd. His research interests are in MEMS and sensors. (hung@nanosys.mech.tohoku.ac.jp)

Haruhiko Asanuma received his B.Sc. and M.Sc. degrees in physics from the Faculty of Science and the Graduate School of Science, Tohoku University, Japan, in 2005 and 2007, respectively. After five years of service in industry, he joined the Graduate School of Engineering, Tohoku University, and received his Ph.D. degree in 2015. He is currently an assistant professor at Kanazawa University, Japan. His research interests include applied material physics, VEHs, and semiactive vibration control. (h-asanuma@se.kanazawa-u.ac.jp)

Hiroyuki Oguchi was born in Shiga Prefecture, Japan in 1975. He obtained his M.Eng. degree from Tokyo University (2002) and his Ph.D. degree from University of Maryland (2008). He was an assistant professor (2008–2012) and has been an associate professor (2012–2020) at Tohoku University. He has worked on growth of films with energy-related functions and their application to energy devices. One representative recent work is the growth of hydride films with fast Li-ion conduction, which will be applied to Li-ion batteries in the future. Another representative work is the growth of AlN-based films and their application to high-power generation VEHs. (oguchi@nanosys.mech.tohoku.ac.jp)

Gaël Sebald received his M.Sc. degree in electrical engineering and his Ph.D. degree in acoustics from INSA Lyon, France, in 2001 and 2004, respectively. He then received a Japan Society for Promotion of Science (JSPS) fellowship for a postdoctoral position at Tohoku University (Sendai, Japan). He became an associate professor in 2005 at INSA Lyon, and a professor in 2016. In 2010, he was a JSPS Invited Researcher in the Department of Nanomechanics at Tohoku University. Since 2016, he has been based in an International Joint Lab between France and Japan at Tohoku University. His research interests are mainly in the understanding of multiphysics coupling in materials, and their application to low-power energy harvesting from temperature and vibration, as well as electrocaloric and electrocaloric cooling materials and applications. He is also working on nonlinear dynamics applied to energy harvesting, ferroelectric/ferromagnetic modeling, and fractional calculus applied to hysteresis dynamics and electromagnetic nondestructive testing. (gael.sebald@insa-lyon.fr)

Hiroki Kuwano received his B.Eng. and M.Eng. degrees in mechanical engineering, and his Ph.D. degree in electrical engineering from Tohoku University, Sendai, Japan, in 1975, 1977, and 1990, respectively. He was a member of the Electrical Communication Laboratories of Nippon Telephone and Telegraph Public Corporation. Since 2003, he has been a professor at Tohoku University. He has authored or co-authored over 120 technical papers and books, and over 50 patents in microelectromechanical systems and particle beam processing. His research interests are in nanoenergy systems, including energy harvesting systems and sensor networks, particularly those used for safety and medical applications.
(hiroki.kuwano@nanosys.mech.tohoku.ac.jp)